ChemComm

COMMUNICATION

View Article Online
View Journal | View Issue

Cite this: *Chem. Commun.*, 2025, **61**, 12147

Received 22nd May 2025,
Accepted 24th June 2025

DOI: 10.1039/d5cc02803e

rsc.li/chemcomm

Hydroxylamine: an overseen intermediate that brings into question nitrogen selectivity in metal-catalyzed nitrate and nitrite reduction†

Janek Betting, Leon Lefferts * and Jimmy Faria Albanese *

In decades of nitrate and nitrite hydrogenation research, nitrite, ammonia, and nitrogen gas were assumed to be the only relevant products. However, we have discovered hydroxylamine on several metal catalysts under various reaction conditions using a simple derivatization strategy based on the oximation of benzaldehyde with hydroxylamine. This previously overlooked intermediate challenges pervasive assumptions of nitrogen gas selectivity and compels a reexamination of the reaction mechanism. Additionally, the hydroxylamine presence represents a major setback for the application of catalytic nitrate and nitrite reduction in drinking water purification.

Nitrogen oxyanions are ubiquitous intermediates in the natural nitrogen cycle, playing a crucial role in sustaining life on Earth. The development of synthetic nitrate fertilizers has been instrumental in supporting global population growth by enabling ammonia synthesis from dinitrogen and hydrogen, which is later oxidized into nitro oxyanions. Unfortunately, the unintended leakage and accumulation of these compounds in the environment pose serious threats to public health due to its toxicity and ecological damage *via* eutrophication of water bodies.[1–7]

In nature, various bacteria—such as those within the *Proteobacteria* phylum—facilitate denitrification in oxygen-deprived environments leveraging nitrate (NO_3^-) and nitrite (NO_2^-) reductase enzymes, provided that sufficient carbon sources are available to drive the metabolic machinery.[1,3] While natural bacteria can contribute to reducing NO_3^- and NO_2^-, the rates achieved through biological denitrification are insufficient to counteract the continuous release of nitrogen oxyanions into the environment.[8,9]

Inspired by natural reductase enzymes, the catalytic reduction of NO_3^- and NO_2^- to N_2 using hydrogen on metals has been proposed as an alternative to bio-based processes. Its simplicity and higher reaction rates have driven extensive research for the past thirty years. This higher activity, however, often comes at the expense of ammonia formation.[10–12] This is highly undesirable due to stringent concentration limits of ammonia (0.5 mg L^{-1}) compared to nitrate (50 mg L^{-1}) in drinking water.[13] Therefore, substantial research has been devoted to developing catalysts with high selectivity to unleash its practical use.

Two distinct catalysts are required for NO_3^- and NO_2^- reduction (see eqn (1)–(3)). While nanoparticles of palladium (Pd) suffice for NO_2^- reduction, bimetallic Pd–Cu, Pd–Sn or Pd–In catalysts arose as best alternatives for NO_3^- reduction.[10,11,14,15]

$$NO_3^- + H_2 \rightarrow NO_2^- + H_2O \quad (1)$$

$$2NO_2^- + 3H_2 + 2H^+ \rightarrow N_2 + 4H_2O \quad (2)$$

$$NO_2^- + 3H_2 + 2H^+ \rightarrow NH_4^+ + 2H_2O \quad (3)$$

The standard procedure to record the reaction rate and product distribution is ion chromatography (IC) or high-performance liquid chromatography (HPLC) to determine NH_4^+, NO_3^- and NO_2^- concentrations. A fundamental assumption in the literature is that no other products are formed and, thus, the remainder in the products is dinitrogen (N_2). Thus, commonly a mass balance closure has not been proven. This method is broadly accepted as closing the mass balance is a major challenge due to (1) N_2 contamination from the surrounding atmosphere is difficult to suppress, (2) the low concentration of gaseous products (*e.g.* NO and N_2O) under typical reaction conditions, and (3) complexity of sampling and quantification of the gas- and liquid phase streams during reaction at the low concentrations of NO_3^- and NO_2^- reactants typically employed (50 ppm). In samples from the stationary liquid phase, the product amounts can be directly calculated, while the gaseous products are dependent on liquid-gas mass transfer, headspace of the reactor and the gas flow rate that continuously flushes out the gaseous products.

Careful inspection of the literature revealed that only very few studies have presented a closed mass balance. Werth *et al.*

Catalytic Processes and Materials Group, Department of Chemical Engineering, Faculty of Science and Technology, MESA+ Institute for Nanotechnology, University of Twente, Enschede 7500 AE, The Netherlands.
E-mail: l.lefferts@utwente.nl, j.a.fariaalbanese@utwete.nl

† Electronic supplementary information (ESI) available. See DOI: https://doi.org/10.1039/d5cc02803e

achieved a closed mass balance over the full reaction time using isotope labelled N species.[16] Vorlop *et al.* analyzed both liquid and gas phases in a batch reaction but missed up to ~30% in the mass balance during the reaction. A closed mass balance could only be achieved by elongating the reaction time by a factor of ~1.5 beyond full NO_3^- and NO_2^- conversion.[17] They suggested that strong adsorption of intermediates on the catalyst and dissolved nitrous oxide acted as reservoirs during the reaction, leading to the incomplete mass balance closure at low conversions. In earlier works, our group also suggested adsorbed intermediates as a reason for an increase of the NH_4^+ concentration after full NO_2^- conversion.[18] Pintar *et al.* mentioned that no NH_2OH was found in a few of their studies[19–21] without presenting any proof to support this claim. Wong *et al.* mentioned NH_2OH as an adsorbed species in their reaction mechanism but assumed that its desorption was not favorable. Thus, NH_2OH as a dissolved intermediate was not reported.[22] The same group detected hydrazine (N_2H_2) over both Pd/Al_2O_3 and Rh/Al_2O_3 catalysts.[23] However, this was observed only at unusually high pH values (>7) where low catalytic activities are recorded, and the maximum yield of hydrazine remained limited to ~1.5% (0.5 ppm in solution).[23] Here, one would wonder if this simplification of the nitrogen mass balance would be of any importance from the scientific and application perspective. In the present contribution, we challenge this postulate and explore if other relevant species beyond NO_2^-, NH_4^+ and N_2 are formed during the reaction.

To address this question, we conducted a series of experiments using Pd-based catalysts for the reduction of NO_3^- and NO_2^- in aqueous environments and quantified NH_2OH. Measuring NH_2OH, however, is not trivial. This species can undergo degradation at high pH.[24,25] Fortunately, hydroxylamine reacts quantitatively with aldehydes, ketones, and acids. These reactions are fast, chemoselective, and thermodynamically favorable at room temperature, making them an attractive proxy for the NH_2OH formation during NO_3^- and NO_2^- reduction. In fact, Lee *et al.* leveraged this chemistry to produce benzaldehyde oxime from benzaldehyde using NO_3^- and NO_2^- as a N-source over nanoscale zero-valent iron, which is only possible if NH_2OH is formed during the reaction.[26] While *in situ* C–N bond formation from NO_3^- and NO_2^- was not followed in thermo-catalysis, it is an emerging research field in electrocatalysis.[27–29]

To detect and quantify NH_2OH, we added 1 μL benzaldehyde to the liquid aliquot right after sampling the reaction mixture, suppressing decomposition of hydroxylamine to other products than benzaldehyde-oxime (Fig. 1). By using a 5-fold excess of benzaldehyde with respect to the maximal possible NH_2OH concentration, full oximation was realized without significantly changing the sample volume (1.5 mL). As the catalyst is separated from the liquid aliquot to terminate the reaction in the sample, before the benzaldehyde addition, the native product distribution remains unchanged by this strategy. The resulting benzaldehyde oxime can be quantified by liquid chromatography (HPLC) due to its strong UV-vis absorbance at 248 nm (see details in the ESI†).

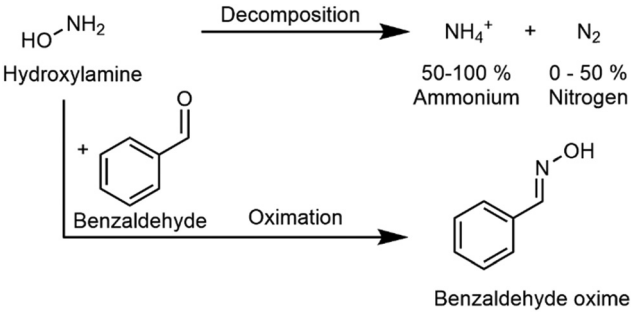

Fig. 1 Aldehyde oximation strategy for detection of NH_2OH intermediates using benzaldehyde in the aqueous phase.

To establish the experimental space in which NH_2OH is formed as a reaction intermediate, we varied the reaction conditions and the catalyst composition in the NO_3^- and NO_2^- hydrogenation. In a typical experiment, carbon dioxide (CO_2) was flushed through the reactor to buffer the media (pH ~ 6), while the temperature was set at room conditions (22 °C), and the nitrate concentration was ~0.8 mM (~50 mg L^{-1} NO_3^-), representing well the reaction conditions widely used in the literature.[10,11,14,15] Fig. 2 illustrates that the NH_4^+ concentration increases with increasing NO_3^- conversion while NO_2^- occurs in trace amounts throughout the entire experiment. Surprisingly, the protocol herein proposed revealed the formation of NH_2OH during the reaction. Notably, the rate of NH_2OH decomposition is slower than that of NO_3^- reduction, leading to substantial NH_2OH accumulation in the system.

The point of full NO_3^- and NO_2^- conversion would typically be considered as the end of the reaction and, therefore, be the reference for determination of NH_4^+ and N_2 selectivity. Since this calculation would disregard NH_2OH formation, the resulting mass balance and the N_2 selectivity would be erroneous. The NH_2OH yield at full NO_3^- and NO_2^- conversion, which we

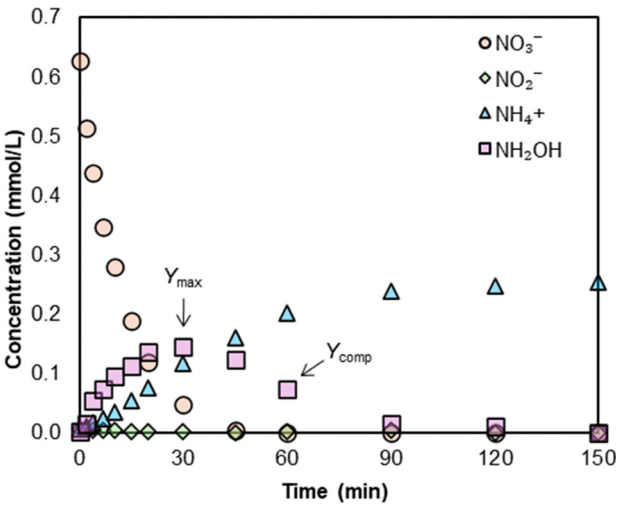

Fig. 2 Typical concentration profile of NO_3^- reduction (entry 6 in Table 1). Reaction conditions: 50 mg $SnPd/Al_2O_3$, 300 mL, 80 : 10 : 10 mL min^{-1} H_2 : CO_2 : He, 600 rpm, and RT.

Table 1 Overview of nitrate and nitrate reduction experiments with several catalysts and conditions with maximum NH_2OH yield (Y_{max}) and NH_2OH yield at full NO_3^-/NO_2^- conversion (Y_{comp}). Bold entries denote the variation with respect to the standard conditions or the previous entry. Catalysts denoted with * and ** are different commercial Pd/A_2O_3 catalysts or based on them

No.	Substrate	Catalyst	C_0/mmol L^{-1}	$H_2:CO_2:He$/mL min^{-1}	T/°C	m_{cat}/mg	Y_{max}	Y_{comp}
1	NO_2^-	Pd/Al_2O_3	0.8	80 : 10 : 10	22	50	34	32
2	NO_2^-	Pd/Al_2O_3	0.8	**20 : 10 : 70**	22	20	17	14
3	NO_2^-	Pd/Al_2O_3	**0.2**	80 : 10 : 10	22	20	56	56
4	NO_2^-	Pd/Al_2O_3	0.8	80 : 10 : 10	**40**	20	9	0
5	NO_2^-	**SnPd/Al_2O_3**	0.8	80 : 10 : 10	22	50	16	16
6	**NO_3^-**	SnPd/Al_2O_3	0.8	80 : 10 : 10	22	50	23	12
7	**NO_2^-**	**Pd/Al_2O_3***	0.8	80 : 10 : 10	22	20	16	10
8	NO_2^-	**Pd/Al_2O_3****	0.8	80 : 10 : 10	22	20	4	4
9	NO_3^-	**Sn**Pd/Al_2O_3**	0.8	80 : 10 : 10	22	100	15	14
10	NO_3^-	**In**Pd/Al_2O_3**	0.8	80 : 10 : 10	22	100	23	14
11	NO_3^-	**Cu**Pd/Al_2O_3**	0.8	80 : 10 : 10	22	100	9	1

report as Y_{comp} quantifies this error. Meanwhile, the maximal yield of NH_2OH (Y_{max}) reflects the interplay between the rates of NO_3^- reduction to NO_2^-, N_2, NH_4^+, and NH_2OH. In this system, a high Y_{max} would suggest that this intermediate is quickly formed during the reaction and subsequently desorbs from the catalyst surface. This fundamental step in the reaction mechanism is neglected in the literature, emphasizing the importance of transient quantification of NH_2OH during the reaction to unravel the fundamental mechanism of NO_3^- and NO_2^- reduction.

Table 1 shows the Y_{max} and Y_{comp} of different catalysts, for NO_3^- as well as NO_2^- reduction, at 40 °C and, to some extent, at varied N : H ratios. While it is true that the fundamental details are not fully understood yet, we here report a ubiquitous phenomenon since NH_2OH was detected in all experiments. The NO_2^- reduction reaction was studied at a typical H_2 partial pressure (0.8 bar, entry 1), as well as at a lower H_2 partial pressure (0.2 bar, entry 2), a lower initial concentration (0.2 mM, entry 3) and an elevated temperature (40 °C, entry 4, Fig. S8, ESI†) resulting in maximal NH_2OH yields that varied between 9 and 56%. Two commercial Pd/Al_2O_3 catalysts were used to confirm that NH_2OH formation is a widely occurring phenomenon and does not arise from custom-prepared catalysts (entries 7 and 8). Doping the Pd/Al_2O_3 catalysts with Sn, In and Cu showed substantial concentration of NH_2OH in the reaction mixtures, reaching maximum yields that varied from 4 to 23% (entries 6, 9–11). More importantly, only in a few experiments the NH_2OH amounts after full NO_3^- and NO_2^- conversion were $\leq$1% (entries 4 and 11). For all other experiments, however, NH_2OH ranged from 4–56%, highlighting the importance of reporting the concentration of this species when reporting catalyst performance. This is especially relevant when applying this for drinking water purification as hydroxylamine is even more toxic than the NO_3^-, NO_2^-, and NH_4^+ counterparts.

The selectivity of the NH_2OH decomposition after full NO_3^- and NO_2^- conversion in the presence of H_2 is important as it can lead to higher NH_4^+ concentrations, which is highly undesirable in drinking water. The NH_2OH decomposition can either proceed *via* catalytic hydrogenation resulting in 100% NH_4^+ or *via* catalytic disproportionation resulting in the 1 : 1 formation of N_2 and NH_4^+.[30]

$$NH_3OH^+ + H_2 \rightarrow NH_4^+ + H_2O \quad (4)$$

$$4NH_2OH + 2H^+ \rightarrow 2NH_4^+ + N_2O + 3H_2O \quad (5)$$

The formed N_2O under reaction conditions is quickly converted to N_2.[16] The same cannot be said about NH_2OH. When decomposition experiments of hydroxylamine were conducted in the absence of a catalyst and any NO_3^- or NO_2^-, the observed reaction rates were negligible (Fig. S7, ESI†). In stark contrast, in the presence of a catalyst substantial hydroxylamine conversion was observed (Fig. S9 and S10, ESI†). To visualize this one could compare the concentration increase of NH_4^+ due to the conversion of hydroxylamine, after completion of the NO_3^- and NO_2^- conversion. As shown in Fig. 3, two lines can be plotted to indicate the NH_4^+ concentrations that would be obtained if the conversion takes place *via* either hydrogenation (100% selectivity NH_4^+) or disproportionation (50% selectivity NH_4^+). The data points spread in-between both boundaries indicating that both hydrogenation and disproportionation contribute (see the source data Table S2, ESI†). While it is true that in these experiments the extent of NH_2OH conversion was different for each data point, the results suggest a complex interplay between the NH_4^+ and N_2 formation. Here, one may hypothesize that a major part of the NH_4^+ formed during NO_3^- and NO_2^- reduction is generated *via* a NH_2OH intermediate owing

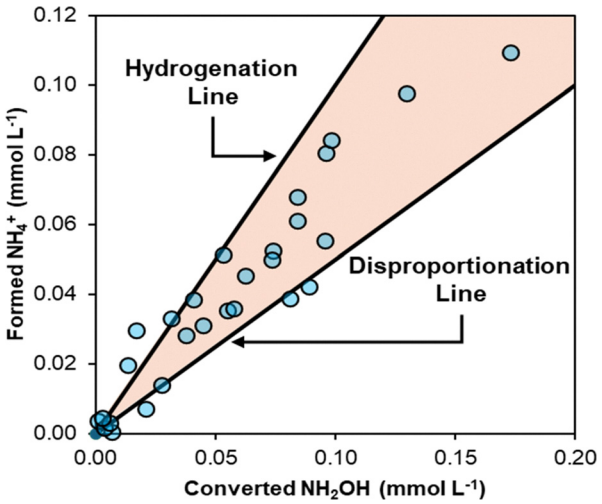

Fig. 3 Amount of NH_4^+ formed in relation to the amount of NH_2OH converted upon full conversion of NO_3^- and NO_2^- for experiments 1 to 11.

to the high NH_4^+ selectivity of the NH_2OH decomposition. Considering that NH_4^+ formation is the major roadblock for widespread implementation of this technology in drinking water purification, it is crucial to consider NH_2OH in the catalyst and process design as well as in mechanistic studies.

In this study, we have shown unequivocal evidence that hydroxylamine is an essential intermediate product in the reduction of NO_3^- and NO_2^- in aqueous environments. These results have profound implications on the calculation of selectivity to N_2 based on the concentrations of NO_3^-, NO_2^- and NH_4^+ exclusively. More importantly, this discovery reshapes our understanding of this critical reaction and provides a simple and accurate strategy for hydroxylamine quantification *via* oximation that is relevant for thermo-catalytic and potentially enzymatic processes[31,32] for nitrogen oxyanions reduction in aqueous environments.

Conflicts of interest

There are no conflicts to declare.

Data availability

The data supporting this article have been included as part of the ESI.†

Notes and references

1 M. Hu, Y. Liu, Z. Yao, L. Ma and X. Wang, *Front. Environ. Sci. Eng.*, 2018, **12**, 1–18.
2 WHO, *Guidelines for drinking-water quality*, 2022.
3 A. J. Lecloux, *Catal. Today*, 1999, **53**, 23–34.
4 D. E. Canfield, A. N. Glazer and P. G. Falkowski, *Science*, 1979, **2010**(330), 192–196.
5 U. Prüsse, M. Hähnlein, J. Daum and K.-D. Vorlop, *Catal. Today*, 2000, **55**, 79–90.
6 K. N. Heck, S. Garcia-Segura, P. Westerhoff and M. S. Wong, *Acc. Chem. Res.*, 2019, **52**, 906–915.
7 C. S. Bruning-Fann and J. B. Kaneene, *Vet. Hum. Toxicol.*, 1993, **35**, 521–538.
8 J. S. Stamler, D. J. Singel and J. Loscalzo, *Science*, 1979, **1992**(258), 1898–1902.
9 J. N. Galloway, A. R. Townsend, J. W. Erisman, M. Bekunda, Z. Cai, J. R. Freney, L. A. Martinelli, S. P. Seitzinger and M. A. Sutton, *Science*, 1979, **2008**(320), 889–892.
10 G. Tokazhanov, E. Ramazanova, S. Hamid, S. Bae and W. Lee, *Chem. Eng. J.*, 2020, **384**, 123252.
11 I. Sanchis, E. Diaz, A. H. Pizarro, J. J. Rodriguez and A. F. Mohedano, *Sep. Purif. Technol.*, 2022, **290**, 120750.
12 F. Ruiz-Beviá and M. J. Fernández-Torres, *J. Clean Prod.*, 2019, **217**, 398–408.
13 European Union, Directive on the quality of water intended for human consumption, 2020.
14 K. G. N. Quiton, M. C. Lu and Y. H. Huang, *Chemosphere*, 2021, **262**, 128371.
15 J. Martínez, A. Ortiz and I. Ortiz, *Appl. Catal., B*, 2017, **207**, 42–59.
16 R. Zhang, D. Shuai, K. A. Guy, J. R. Shapley, T. J. Strathmann and C. J. Werth, *ChemCatChem*, 2013, **5**, 313–321.
17 U. Prüsse, J. Daum, C. Bock and K.-D. Vorlop, *Stud. Surf. Sci. Catal.*, 2000, **130**, 2237–2242.
18 Y. Zhao, N. Koteswara Rao and L. Lefferts, *J. Catal.*, 2016, **337**, 102–110.
19 A. Pintar, J. Batista and I. Muševič, *Appl. Catal., B*, 2004, **52**, 49–60.
20 A. Pintar and J. Batista, *Appl. Catal., B*, 2006, **63**, 150–159.
21 A. Pintar and J. Batista, *J. Hazard. Mater.*, 2007, **149**, 387–398.
22 H. Li, S. Guo, K. Shin, M. S. Wong and G. Henkelman, *ACS Catal.*, 2019, **9**, 7957–7966.
23 C. A. Clark, C. P. Reddy, H. Xu, K. N. Heck, G. Luo, T. P. Senftle and M. S. Wong, *ACS Catal.*, 2020, **10**, 494–509.
24 Q. Wang, C. Wei, L. M. Pérez, W. J. Rogers, M. B. Hall and M. S. Mannan, *J. Phys. Chem. A*, 2010, **114**, 9262–9269.
25 C. Wei, S. R. Saraf, W. J. Rogers and M. Sam Mannan, *Thermochim. Acta*, 2004, **421**, 1–9.
26 M. A. Kumar, J. K. Choe, W. Lee and S. Yoon, *Environ. Nanotechnol. Monit. Manag.*, 2017, **8**, 97–102.
27 P. Liao, J. Kang, R. Xiang, S. Wang and G. Li, *Angew. Chem., Int. Ed.*, 2024, **63**, 1–12.
28 S. R. Udayasurian and T. Li, *Nanoscale*, 2024, **16**, 2805–2819.
29 C. L. Rooney, Q. Sun, B. Shang and H. Wang, *J. Am. Chem. Soc.*, 2025, **147**, 9378–9385.
30 V. D. Moesdijk, TU Eindhoven, 1979.
31 N. Lehnert, H. T. Dong, J. B. Harland, A. P. Hunt and C. J. White, *Nat. Rev. Chem.*, 2018, **2**, 278–289.
32 N. Jawali, J. K. Saws and P. V. Sane, *Phytochemistry*, 1978, **17**, 1527–1530.

